International Journal of Engineering

Journal Homepage: www.ije.ir

Land Covers Classification from LiDAR-DSM Data Based on Local Kernel Matrix Features of Morphological Profiles

B. Asghari Beirami*, M. Mokhtarzade

Department of Photogrammetry and Remote Sensing, Faculty of Geodesy and Geomatics, K. N. Toosi University of Technology, Tehran, Iran

A B S T R A C T

Accurate land cover classification from the digital surface model (DSM) obtained from LiDAR sensors is a challenging topic that researchers have considered in recent years. In general, the classification accuracy of land covers leads to low accuracy using a single-band DSM image. Hence, it seems necessary to develop efficient methods to extract relevant spatial information, which improves classification accuracy. In this regard, using spatial features based on morphological profiles (MPs) has significantly increased classification accuracy. Despite MPs' efficiency in increasing the DSM's classification accuracy, the classification accuracy results under the situation of limited training samples are not still at satisfactory levels. The main novelty of this paper is to propose a new feature space based on local kernel descriptors obtained from MP for addressing the mentioned challenge of MP-based DSM classification. These innovative feature vectors consider local nonlinear dependencies and higher-order statistics between the morphological features. The experiments of this study are conducted on two well-known DSM datasets of Houston and Trento. Our results show that support vector machine (SVM)-based DSM classification with the new local kernel features achieved an average accuracy of 93.75%, which is much better than conventional SVM classification with single-band DSM and MP features (by about 57% and 11.5% on average, respectively). Additionally, our proposed method outperformed two other DSM classification methods by an average of 4.7%.

doi: 10.5829/ije.2023.36.09c.04

1. INTRODUCTION

Aerial LiDAR is a type of remote sensing sensor that uses laser pulses to measure the distance between the receiver and the earth's surface. Generally speaking, elevation models and 3D point clouds are two important outputs of LiDAR sensors that are used in various fields, including forestry research, geodesy, geology, urban research, and crisis management [1-3]. LiDAR can collect data in all weather and lighting conditions, unlike optical and infrared sensors [4]. LiDAR sensors generate a digital surface model (DSM) as a secondary outcome, which is produced by implementing various techniques like denoising and rasterization on a point cloud. DSM contains elevational data of ground objects, which can be used to distinguish objects of different heights [5].

DSM is typically used as supplemental data to optical or hyperspectral images in order to classify land cover. For instance, Zhang et al. [6] developed a new classification system that categorizes land covers using extinction profiles derived from hyperspectral images and the DSM. The final results of their research show that the integration of spectral features and the DSM increases classification accuracy. Singh et al. [7] introduced a novel deep-learning strategy for classifying land cover using LiDAR and hyperspectral images in their study. The method utilizes sparse stacked autoencoders and morphological profiles, as outlined in literature [7].

Although DSM has been used in several studies as supplementary data, researchers' interest in classifying land covers using a single-band DSM image has recently increased. When few training examples are available,

---

Correponding author Email: b_asghari@email.kntu.ac.ir
(B. Asghari Beirami)

distinguishing between ground cover with only a single-band DSM image results in low accuracy, necessitating the development of more effective techniques. Most alternative approaches hinge on utilizing the spatial and contextual details present in DSM images to enhance classification accuracy, primarily attributable to the superior spatial resolution of LiDAR sensors. One of the primary spatial features used by numerous studies to categorize the DSM image is morphological profiles (MPs). To classify land cover from LiDAR data, Ghamisi and Hoefle [8] proposed a composite kernel SVM classification method based on extinction profiles. Their research culminated in a classification accuracy of roughly 87% for DSM images from the University of Houston dataset. In a separate research project, Wang and colleagues [4] suggested a new approach to DSM image classification utilizing the combination of morphological profiles and deep convolutional networks. He et al. [9] evaluated the performance of spatial transformer networks in integration with morphological features to classify the DSM image after demonstrating the efficiency of deep learning methods in classifying LiDAR data. Transformer networks outperform traditional convolutional neural networks, according to their final findings. A step forward in this direction was taken by Wang and colleagues [10], who developed a superior model for DSM data classification through the integration of dense convolutional neural networks and spatial transformer networks.

According to the literature, deep neural networks underlie the majority of the proposed methods for classifying DSM images, but it should be noted that using deep models comes with its own challenges. For instance, using deep models necessitates tuning thousands or even millions of parameters and involves computational complexity. Some expensive, high-end hardware, such as GPUs, is required to adjust this enormous number of parameters. On the other hand, overfitting, a condition that reduces these networks' effectiveness, is possible when few training samples are available. Therefore, developing accurate, quick, and shallow methods seem necessary.

Recent research in machine vision has shown that using covariance descriptors, which consider linear dependencies, can improve the performance of machine learning techniques on certain tasks, such as face recognition [11]. A more general form of covariance descriptor is the kernel descriptor, which typically performs better than covariance by considering nonlinear dependencies between features and higher-order statistics [12, 13]. In this regard, in remote sensing, Beirami and Mokhtarzade [14] developed local kernel features for classifying hyperspectral images and proving

the efficiency of nonlinear relationships between spectral features in the classification of hyperspectral images. Despite demonstrating the efficiency of local kernel features, their efficiency in increasing the classification accuracy of DSM images is still unknown. In view of the potential of local kernel features to enhance the accuracy of land cover classification, a novel method for extracting features is introduced herein for DSM image classification. The novel feature space put forth in this study takes into account the nonlinear dependences and higher-order statistics between morphological features. For this purpose, in this study, after generating spatial features using MP, local kernel features were generated from them and then fed to machine vector machines (SVM) classifier for classification.

Our motivation for proposing a new DSM classification method based on local kernel matrix features is twofold. First, these features have shown great performance in other fields of image processing, such as hyperspectral image classification [15], particularly in situations with limited training sample sizes. Second, producing these local kernel matrix features is straightforward and does not require advanced hardware, such as GPUs, unlike some other DSM classification methods.

The main novelty of this paper is the introduction of robust and efficient kernel features derived from morphological features for DSM image classification. These new features are expected to significantly improve the classification accuracy of DSM images due to their ability to consider nonlinear dependencies between morphological features.

The present paper is structured as follows: In the second section of this study after introducing the DSM datasets used in this study, we describe the proposed DSM classification approach in detail. In the third section, we report and analyze the classification results. Lastly, we conclude our research in the final section before discussing future study plans.

2. THE PROPOSED APPROACH

In this section, we introduce the dataset used in our study and describe the methodology employed.

2. 1. Datasets   Researchers in the IEEE competition employed the Houston dataset as a reference collection, which was gathered from the University of Houston campus in 2012. The dataset includes a LiDAR-captured DSM with a density of one point in 2.5 meters and a ground truth map consisting of 15 urban classes such as buildings, water, soil, trees, and roads. Figure 1 depicts the DSM image of the Houston University region.

Figure 1. Houston University LiDAR-DSM

The Trento DSM dataset was acquired by Optech ALTM 3100EA sensor over a rural region located in the southern part of Trento, Italy. The dataset, which comprises 166×600 pixels, has been captured with a spatial resolution of 1m. The Trento dataset has six distinct categories, namely apple trees, buildings, ground, wood, vineyard, and roads. Figure 2 represents the Trento DSM image.

2. 2. Methodology   In this subsection, the proposed DSM classification method is introduced after reviewing some related basic concepts.

2. 2. 1. Morphological Profiles   Morphological profiles are among the most significant spatial features used to categorize DSM images, as was already mentioned. MPs generally improve classification accuracy because of their high ability to extract geometric properties of objects and classes. MP is built upon two fundamental morphological operators, namely opening (OP) and closing (CL). These operators are established using the essential erosion (•) and dilation (∘) operators, with the following definitions [16]:

$$OP = (A \bullet B) \circ B \tag{1}$$

$$CL = (A \circ B) \bullet B \tag{2}$$

A DSM image with only one band is denoted as A, while B symbolizes a structuring element (SE) in the equations mentioned earlier. To capture the intricate geometric details of objects, present within the DSM image that come in varying sizes, morphological attributes are generated utilizing SEs of diverse sizes. As a result, if we represent the dimensions of the structural element as L, an MP can be displayed as follows:

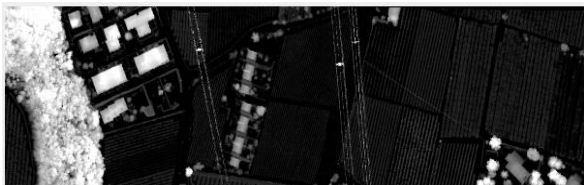$$MP = [OP_L, OP_{L-1}, \ldots, A, \ldots, CL_{L-1}, CL_L] \tag{3}$$

Figure 2. Trento LiDAR-DSM

In the center of an MP lies the primary DSM image, while its sides showcase DSM images that have undergone size-varied structural element operations of opening and closing. The use of disc-shaped SEs is more frequent for creating MPs, according to the research background, because of its isotropic behavior in all directions.

2. 2. 2. Local Kernel Matrix Features   By calculating higher-order statistics and nonlinear relationships between features, the local kernel matrix can offer significant improvements in classification accuracy. To illustrate, suppose we have an image with N bands, and we examine a window of size $l \times l$ (containing R pixels) centered around each pixel. We compute every element of the local kernel matrix using the following formula:

$$k(y_i, y_j) = \exp(-\beta \|y_i - y_j\|^2) \tag{4}$$

where y is the vector with size R, which contains the grey-level values of pixels in the local $l \times l$ window, indices i and j represent the ith and j^{th} bands, and β is the scaling parameter of the radial basis function, which is set to 1 in this study by experiment. Since calculating the k in the fixed window size may bias the final results, similar to work conducted by Mirzapour, and Ghassemian [17]. This paper uses a weighted version of Equation (4) for feature generation. To do so, the weight of each pixel in coordinate (r,c) in the local $l \times l$ window is represented by:

$$P = \sqrt{r^2 + c^2} \tag{5}$$

$$weight (r,c) = 1/(P + 1) \tag{6}$$

To prevent infinity, Equation (6) employs 1 in the denominator. Following the computation of pixel weights within the local $l \times l$ window, the weighted form of Equation (4) can be expressed as follows [14]:

$$k(y_i, y_j) = \exp(-\|Wy_i - Wy_j\|^2) \tag{7}$$

The vector W consists of weights assigned to every pixel in the $l \times l$ local window. Finally, after calculating k for each pair of features, a weighted local kernel matrix (WLKM) with size N×N is calculated by Beirami, and Mokhtarzade [15]:

$$K = \begin{bmatrix} k(y_1, y_1) & \ldots & k(y_1, y_N) \\ \vdots & \ddots & \vdots \\ k(y_N, y_1) & \ldots & k(y_N, y_N) \end{bmatrix} \tag{8}$$

After calculating the WLKMs in the form of equation (8) for each pixel, to further improve the quality of extracted features, the matrix logarithm operator is applied to WLKMs as [16]:

$$logm(K) = U log(\Sigma) U^T \tag{9}$$

The eigen-decomposition of Matrix K is used to compute U and Σ. Subsequently, upper or lower triangular elements from $logm(K)$ serve as the WLKM features. The size of the resulting feature vectors is $N \times (N+1)/2$, with a total of 325 WLKM features generated (which equals $(25 \times 26)/2$, where 25 denotes the number of MP features).

2. 2. 3. Proposed Method   This study aims to evaluate the potential improvement in the classification accuracy of DSM images through the integration of WLKM features that have been extracted from MP. A block diagram demonstrating the suggested technique is depicted in Figure 3. Essentially, the methodology put forth in this study consists of three pivotal phases:

1) In the first step, morphological profiles are created from a single-band DSM image using equation (3). The use of MP, which contains geometric information, enhances classification accuracy.

2) In the second step, the generated features from step 1 are given as input to the WLKM feature generation method. This method can generate features that contain nonlinear dependencies and high-order statistics of MP features.

3) In the third stage, the feature vectors generated from the second stage are classified by the SVM classifier using training samples. Finally, the accuracy of classification is evaluated using test samples.

This study's suggested technique is primarily evaluated against two fundamental methodologies. these approaches are based on the SVM classification of single-band DSM and the SVM classification of MP features.
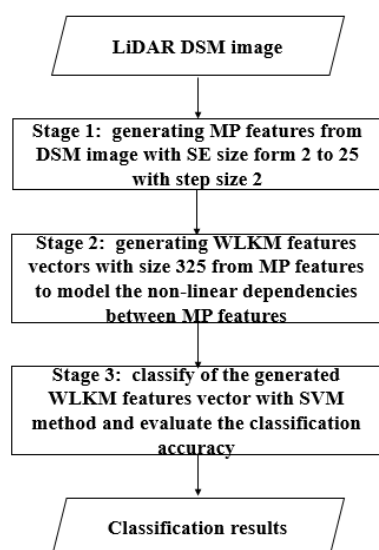

Figure 3. Block diagram of the proposed method

3. EXPERIMENTAL RESULTS

The suggested algorithm was put into practice using the two mentioned DSM datasets. From the ground truth maps of each dataset, training samples are randomly chosen in two sizes: 40 samples per class (case 1) and 80 samples per class (case 2), with the remaining samples serving as test samples to evaluate the classification accuracy. In our study, we utilized the cross-validation technique to adjust the SVM classification parameters. Our assessment of the classification accuracy involved calculating three metrics from the confusion matrix: overall accuracy (OA), average accuracy (AA), and kappa coefficient (k). To ensure statistical significance, we replicated all experiments ten times and calculated the average outcomes. MATLAB 2020b was employed for implementation on a Core i5 4590 3.3GH processor with 8 GIG RAM, with no inclusion of GPU.

3. 1. Experiments on the Houston Dataset

3. 1. 1. Simulation Details   To classify DSM, our approach uses three key settings: the MP feature dimension, β in equation 4, and the window size for the WLKM method. We've set the MP dimension to 25 by creating MP with SE sizes ranging from 2 to 25 (in increments of 2). We've also set β to 1. To choose these values, we used trial and error, prioritizing speed and accuracy. To determine the optimum window size of the WLKM method, SVM classification is conducted with Figure 4 presents the classification outcomes for several window sizes (5 to 15) in the initial test of this subsection, which examines the final classification outcomes of the WLKM feature generation method in relation to window size. The results propose window size 13 as the optimal selection for maximum accuracy. Accuracy drops slightly after window size 13, as demonstrated in Figure 4. Although the automatic detection of window size is an interesting topic that will be investigated in future studies, using any window size between 5 and 15 can obtain better results than MP-based classification.
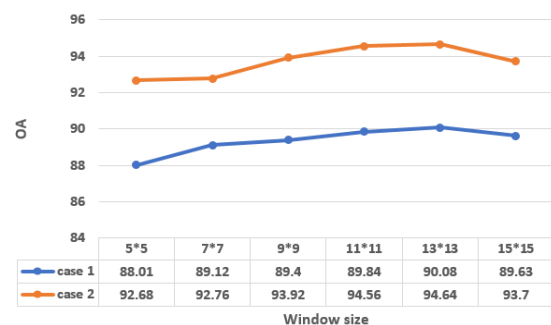

	5*5	7*7	9*9	11*11	13*13	15*15
case 1	88.01	89.12	89.4	89.84	90.08	89.63
case 2	92.68	92.76	93.92	94.56	94.64	93.7

Figure 4. Impact of window size on classification accuracy of WLKM features

3. 1. 2. Analysis of Classification Results   As stated earlier, the proposed WLKM DSM classification method is basically compared with DSM-based and MP-based classification methods. Classification results on each case of training ratio are shown in Table 1. Figure 5 also displays each method's classified images under case 1 of the training sample.

Below are the key results obtained from these experiments:

- It can be understood that local nonlinear dependencies improve the classifier's performance and reduce noise in the classified image. This means that the new WLKM feature vectors of each pixel are similar within the same class and different across different classes.
- Table 1 shows that the classification accuracy of DSM images is very poor (OAs are below 30%), and Figure 5(a) shows that the classified images are very noisy. As a result, the classified maps produced using only the DSM image are not very accurate. Table 1 displays an intriguing finding that increasing

TABLE 1. The Houston dataset's classification outcomes compared across various techniques

Accuracy criteria	Training ratio	Methods		
		DSM	MP	WLKM
OA		22.8	81.64	**90.08**
AA	Case 1	35.26	83.48	**91.43**
K×100		23.73	79.92	**89.12**
OA		28.97	77.25	**94.64**
AA	Case 2	36.04	78.99	**95.46**
K×100		24.32	75.1	**94.1**

(a)

(b)

(c)
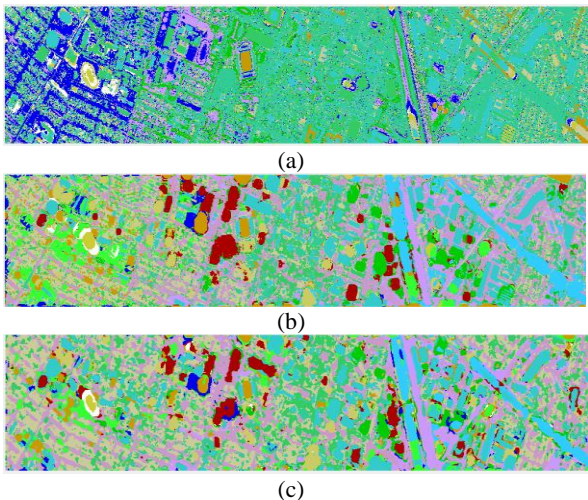
Figure 5. Classified images (a) DSM feature (b) MP features (c) WLKM features

the sample size from 40 to 80 does not lead to a notable improvement in classification accuracy.

- As seen from Table 1, compared to DSM-based classification, using spatial features of MP can hugely increase the classification accuracy by about 50%. Furthermore, classified maps obtained from MP features are smoother than classified images of the previous experiment, as shown in Figure 5(b). Table 1 shows that, similarly to the previous finding, increasing the size of training samples cannot improve classification accuracy.
- According to Table 1, the proposed method based on WLKM features provides the most accurate classified images. Table 1 shows that even with very few training samples, the proposed WLKM-based classification of DSM can still achieve above 90% accuracy (case 1). The image depicted in Figure 5(c) illustrates the smoother and more refined classified image obtained through the utilization of the proposed WLKM approach. Unlike the previous two findings, this method showcased an improvement in classification results by increasing the size of training samples. The effectiveness of WLKM features was demonstrated by their potential to consider nonlinear dependencies and higher-order statistics, which proved highly beneficial in accurately classifying images.

3. 1. 3. Comparison to other DSM Classification Methods   As a result of the limited availability of alternative methodologies and the absence of codes for such approaches, the comparison of the DSM classification method proposed on the basis of WLKM has been restricted to only two state-of-the-art (SOTA) methods. Below are some supplementary descriptions pertaining to these techniques:

- MAP-CNN-SiLU [4]: In this method, morphological and multiattribute profiles are combined with a deep CNN with sigmoid-weighted linear units (SiLU) as activation functions to classify DSM images.
- MP-STN [9]: This method combines MPs with spatial transformation CNN for DSM classification. Using a spatial transformation network (STN), this approach identifies the best CNN inputs.

The classification outcomes of each technique are displayed in Table 2. The results are obtained from the authors' primary literature and compared to those for the WLKM-based method that was suggested.

Table 2 demonstrates that our DSM classification method outperforms the other two methods in competition. One way to express the complexity of the suggested approach is by using the subsequent formula:

$$O(proposed)= O(MP)+O(WLKM)+O(SVM) \qquad (10)$$

TABLE 2. Comparison of suggested methodology and two advanced DSM classification techniques

	MAP-CNN-SiLU		MP-STN		proposed	
	Case1	Case2	Case1	Case2	Case1	Case2
OA	83.22	90.71	86.87	92.87	**90.08**	**94.64**
AA	85.94	91.92	89.15	94.18	**91.43**	**95.46**
K×100	81.88	89.95	85.80	92.28	**89.12**	**94.10**

In which O(X) is the computational complexity of the method X. Computation time of the proposed method on the Houston dataset is about 280 seconds, much faster than some other DSM classification methods such as MAP-CNN-SiLU with 642.09 seconds, as reported in their paper. To sum up, our shallow method for DSM classification, as opposed to the other two deep learning methods, employs a simpler structure that enhances its effectiveness.

3. 2. Experiments on the Trento Dataset Assessing the WLKM-based classification technique on the Trento DSM dataset is the objective of our second experiment. Due to the unavailability of results of the previously mentioned SOTA for the Trento dataset, we only report the results of two basic approaches. Classification accuracies of DSM-based and MP-based and WLKM-based classification methods are shown in Table 3 for two cases of training ratio.

The efficiency of the proposed method on the second DSM dataset was confirmed by the ultimate findings of Table 1. On average, the WLKM approach outperformed the MP-based method by approximately 9.72%.

TABLE 3. The Trento dataset's classification outcomes compared across various techniques

Accuracy criteria	Training ratio	Methods		
		DSM	MP	WLKM
OA		45.80	82.83	**93.42**
AA	Case 1	42.47	80.19	**93.47**
K×100		34.05	77.82	**91.25**
OA		49.40	87.97	**96.83**
AA	Case 2	44.32	84.57	**96.89**
K×100		37.39	84.07	**95.75**

4. CONCLUSIONS

The classification of DSM images is addressed in this manuscript by means of a new method. The proposed

approach makes use of local kernel matrix features, which are generated from MP features. The proposed method generates MP features containing pixel spatial and geometric characteristics in the first stage. The next step involves generating WLKM features from the MP features. Ultimately, the SVM classifier is applied to categorize the WLKM features that were extracted. By adopting the WLKM-based DSM classification technique, an accuracy rate of more than 90% can be attained, even when working with limited training samples. In subsequent work, we will develop a new WLKM-based method for fusing hyperspectral data with LiDAR data. Future studies will also examine the effectiveness of WLKM features generated from multishape MP features for DSM classification.

5. ACKNOWLEDGMENT

6. REFERENCES

1. Sharma, M., Garg, R.D., Badenko, V., Fedotov, A., Min, L. and Yao, A., "Potential of airborne lidar data for terrain parameters extraction", *Quaternary International*, Vol. 575, (2021), 317-327. https://doi.org/10.1016/j.quaint.2020.07.039

2. Li, X., Chen, W.Y., Sanesi, G. and Lafortezza, R., "Remote sensing in urban forestry: Recent applications and future directions", *Remote Sensing*, Vol. 11, No. 10, (2019), 1144. https://doi.org/10.3390/rs11101144

3. Muhadi, N.A., Abdullah, A.F., Bejo, S.K., Mahadi, M.R. and Mijic, A., "The use of lidar-derived dem in flood applications: A review", *Remote Sensing*, Vol. 12, No. 14, (2020), 2308. https://doi.org/10.3390/rs12142308

4. Wang, A., He, X., Ghamisi, P. and Chen, Y., "Lidar data classification using morphological profiles and convolutional neural networks", *IEEE Geoscience and Remote Sensing Letters*, Vol. 15, No. 5, (2018), 774-778. https://doi.org/10.1109/LGRS.2018.2810276

5. Wang, A., Xue, D., Wu, H. and Gu, Y., "Efficient convolutional neural architecture search for lidar dsm classification", *IEEE Transactions on Geoscience and Remote Sensing*, Vol. 60, (2022), 1-17.. https://doi.org/10.1109/TGRS.2022.3171520

6. Zhang, M., Ghamisi, P. and Li, W., "Classification of hyperspectral and lidar data using extinction profiles with feature fusion", *Remote Sensing Letters*, Vol. 8, No. 10, (2017), 957-966. https://doi.org/10.1080/2150704X.2017.1335902

7. Singh, M.K., Mohan, S. and Kumar, B., "Fusion of hyperspectral and lidar data using sparse stacked autoencoder for land cover classification with 3d-2d convolutional neural network", *Journal of Applied Remote Sensing*, Vol. 16, No. 3, (2022), 034523-034523. https://doi.org/10.1117/1.JRS.16.034523

8. Ghamisi, P. and Hoefle, B., "Lidar data classification using extinction profiles and a composite kernel support vector machine", *IEEE Geoscience and Remote Sensing Letters*, Vol. 14, No. 5, (2017), 659-663. https://doi.org/10.1109/LGRS.2017.2669304

9. He, X., Wang, A., Ghamisi, P., Li, G. and Chen, Y., "Lidar data classification using spatial transformation and cnn", *IEEE Geoscience and Remote Sensing Letters*, Vol. 16, No. 1, (2018), 125-129. https://doi.org/10.1109/LGRS.2018.2868378.

10. Wang, A., Wang, M., Jiang, K., Zhao, L. and Iwahori, Y., "A novel lidar data classification algorithm combined densenet with stn", in IGARSS 2019-2019 IEEE International Geoscience and Remote Sensing Symposium, IEEE. (2019), 2483-2486.

11. Asghari Beirami, B. and Mokhtarzade, M., "Ensemble of log-euclidean kernel svm based on covariance descriptors of multiscale gabor features for face recognition", *International Journal of Engineering, Transactions B: Applications*, Vol. 35, No. 11, (2022), 2065-2071. https://doi.org/10.5829/IJE.2022.35.11B.01

12. Wang, L., Zhang, J., Zhou, L., Tang, C. and Li, W., "Beyond covariance: Feature representation with nonlinear kernel matrices", in Proceedings of the IEEE international conference on computer vision. (2015), 4570-4578.

13. Zhang, J., Wang, L., Zhou, L. and Li, W., "Beyond covariance: Sice and kernel based visual feature representation", *International Journal of Computer Vision*, Vol. 129, (2021), 300-320. https://doi.org/10.1007/s11263-020-01376-1

14. Beirami, B.A. and Mokhtarzade, M., "Optimized weighted local kernel features for hyperspectral image classification", *Multimedia Tools and Applications*, Vol. 81, No. 15, (2022), 21859-21885. https://doi.org/10.1007/s11042-022-12452-8.

15. Asghari Beirami, B. and Mokhtarzade, M., "Spatial-spectral classification of hyperspectral images based on extended morphological profiles and guided filter", *Computer and Knowledge Engineering*, Vol. 2, No. 2, (2020), 2-8. https://doi.org/10.22067/CKE.V2I2.81519

16. Fang, L., He, N., Li, S., Plaza, A.J. and Plaza, J., "A new spatial–spectral feature extraction method for hyperspectral images using local covariance matrix representation", *IEEE Transactions on Geoscience and Remote Sensing*, Vol. 56, No. 6, (2018), 3534-3546. https://doi.org/10.1109/TGRS.2018.2801387

17. Mirzapour, F. and Ghassemian, H., "Moment-based feature extraction from high spatial resolution hyperspectral images", *International Journal of Remote Sensing*, Vol. 37, No. 6, (2016), 1349-1361. https://doi.org/10.1080/2150704X.2016.1151568

Persian Abstract

چکیده

طبقه بندی دقیق پوشش زمین از مدل سطح دیجیتال (DSM) به دست آمده از سنجنده LiDAR یک موضوع چالش برانگیز است که محققان در سال های اخیر در نظر گرفته اند. به طور کلی، دقت طبقه‌بندی پوشش‌های زمین منجر به دقت پایین با استفاده از یک تصویر DSM تک باندی می‌شود. از این رو، به نظر می رسد توسعه روش های کارآمد برای استخراج اطلاعات مکانی مرتبط، که دقت طبقه بندی را بهبود می بخشد، ضروری به نظر می رسد. در این راستا، استفاده از ویژگی‌های مکانی مبتنی بر نیمرخ‌های مورفولوژیکی (MPs) دقت طبقه‌بندی را به‌طور چشمگیری افزایش داده است. علیرغم کارایی نیمرخ‌های مورفولوژیکی در افزایش دقت طبقه بندی DSM، نتایج دقت طبقه بندی تحت شرایط نمونه های آموزشی محدود هنوز در سطح رضایت بخشی نیست. نوآوری اصلی این مقاله، پیشنهاد یک فضای ویژگی جدید بر اساس توصیفگرهای هسته محلی به‌دست‌آمده از MP برای حل کردن چالش ذکر شده طبقه‌بندی DSM مبتنی بر MP است. این بردارهای ویژگی نوآورانه وابستگی های غیرخطی محلی و آمار مرتبه بالاتر بین ویژگی های مورفولوژیکی را در نظر می‌گیرند. آزمایشات این مطالعه بر روی دو مجموعه داده DSM معروف هیوستون و ترنتو انجام شده است. نتایج نهایی نشان می‌دهد که طبقه‌بندی DSM مبتنی بر SVM با ویژگی‌های هسته محلی جدید به دقت متوسط ۹۳.۷۵ درصد دست یافته است که بسیار بهتر از طبقه‌بندی SVM معمولی با ویژگی‌های تک باند DSM و MP است (به طور متوسط حدود ۵۷ درصد و ۱۱.۵ درصد، به ترتیب). علاوه بر این، روش پیشنهادی این پژوهش به طور متوسط ٤.۷٪ از دو روش طبقه بندی DSM دیگر موجود در پیشینه تحقیق بهتر عمل کرده است.